CHALMERS
UNIVERSITY OF TECHNOLOGY

Effect of Thermal Treatment on Ligno-Boost Lignin

Aiming at understanding the reasons for improved filtration properties

HAMPUS JOHANSSON &
HENRIK SARGE

DEPARTMENT OF CHEMISTRY AND CHEMICAL ENGINEERING
CHALMERS UNIVERSITY OF TECHNOLOGY
Gothenburg, Sweden 2024
www.chalmers.se

Master's thesis 2024

Effect of Thermal Treatment on LignoBoost Lignin

Aiming at understanding the reasons for improved filtration properties

HAMPUS JOHANSSON &
HENRIK SARGE

CHALMERS
UNIVERSITY OF TECHNOLOGY

In collaboration with
Stora Enso & Valmet
Department of Chemistry and Chemical Engineering
Chalmers University of Technology
Gothenburg, Sweden 2024

HAMPUS JOHANSSON & HENRIK SARGE

Supervisors: Anders Littorin, Valmet
Hanna Karlsson, Valmet
Liyang Liu, Chalmers
Merima Hasani, Chalmers
Rickard Wadsborn, Stora Enso
Examiner: Merima Hasani, Chalmers

Master's Thesis 2024
Department of Chemistry and Chemical Engineering
Chalmers University of Technology
SE-412 96 Gothenburg
Telephone +46 31 772 2996

Cover: Lignin-containing plant growing from a lush bed of moss, which does not contain lignin. This imagery powerfully symbolizes how the presence of lignin can be leveraged to achieve growth and elevation, metaphorically suggesting that embracing lignin as a valuable resource can enable us to surpass our current limits and reach new heights.

Typeset in LaTeX
Printed by Chalmers Reproservice
Gothenburg, Sweden 2024

Effect of Thermal Treatment on LignoBoost Lignin
Aiming at understanding the reasons for improved filtration properties
Hampus Johansson & Henrik Sarge
Department of Chemistry and Chemical Engineering
Chalmers University of Technology

Abstract

Transforming lignin into valuable products that can substitute fossil-based materials is crucial for the economic viability of lignocellulosic biorefineries, further enhancing their role in the shift towards a more sustainable world. The LignoBoost process, which extracts lignin from kraft pulp mill black liquor, has been modified by incorporating a thermal treatment step during the final acidification phase. This study investigates the impact of thermal treatment on the filtration properties of LignoBoost lignin, focusing on changes in colloidal properties and structural features. Lignin samples were treated at various temperatures (55, 75, 85, and 95°C) and characterized in terms of particle size distribution (PSD), particle shape, surface charge, molecular weight, molecular structure, and glass transition temperature (T_g). Results indicate that thermal treatment influences both structural and colloidal properties of lignin by increasing degree of condensation and consequently also molecular weight, along with increasing particle size and decreasing surface charge, thereby improving filtration efficiency. The findings provide valuable insights for optimizing the LignoBoost process, ultimately enhancing the utilization of lignin in industrial applications.

Keywords: lignin, LignoBoost, softwood, thermal treatment, filtration, characterization, NMR, zeta potential, particle size distribution

Acknowledgements

We would like to extend our heartfelt gratitude to our supervisors Merima Hasani, Liyang Liu, Hanna Karlsson, Anders Littorin, and Rickard Wadsborn, for your tireless commitment to our work and the success of this project. Thank you for all the valuable and insightful feedback, and for putting our educational journey as a top priority. This project has been an excellent opportunity to apply all the skills we have acquired over our five years at Chalmers, serving as a fitting conclusion to this chapter of our lives.

Hampus Johansson & Henrik Sarge, Gothenburg, May 2024

List of Acronyms

Below is the list of acronyms that have been used throughout this thesis listed in alphabetical order:

DSC	Differential scanning calorimetry
FBRM	Focused beam reflectance measurement
GPC	Gel permeation chromatography
HSQC	Heteronuclear single quantum coherence
M_n	Number average molecular weight
M_w	Weight average molecular weight
NMR	Nuclear magnetic resonance
PSD	Particle size distribution
SLRP	Sequential liquid-lignin recovery and purification
T_g	Glass transition temperature
TGA	Thermal gravimetric analysis
UV-Vis	Ultraviolet-visible

Contents

List of Figures

List of Tables

1
Introduction

Approximately half a billion years ago, the transition of plants from aquatic algae to terrestrial forms marked the establishment of the foundation for life on land. However, the true dominance of land plants in terrestrial ecosystems came with the ascent of tracheophytes, commonly known as vascular plants. These plants had acquired the ability to synthesize and incorporate one important macromolecule into their cell walls: lignin. Lignin played a pivotal role by imparting physical rigidity to the early tracheophytes, allowing them to stand upright, reinforcing the water-conducting cells for efficient long-distance water transport, as well as providing a defensive barrier against co-evolving pathogens and herbivores [1]. The adaptation of lignin was hence the key for larger plants like grasses, bushes, and perhaps most importantly, trees, to evolve.

Lignin, from the latin *Lignum* for wood, is one of the most abundant biopolymers on Earth, only second to cellulose, and is found in the cell wall of almost all terrestrial plants. Its structure is one of the most complex among naturally occurring polymers with a large structural variation, thus difficult to process into lucrative products [2]. As of 2020, the annual global production of industrial lignin exceeded 50 million tons, primarily derived from pulping and bioethanol processes. Despite this substantial output, the utilization of lignin remains significantly limited. Approximately 95% of produced lignin is incinerated for heat and power generation, with the remaining 5% finding application in potential uses such as surfactants, additives, binders, and dispersants. The restrained utilization of lignin stems from large structural variations depending on both the biological source and the extraction process, leading to differences in material properties and processability, rendering it commercially impractical [3]. Hence, transforming lignin intermediates into valuable chemicals represents a key approach to make lignocellulosic biorefineries financially viable. Since lignin from lignocellulosic biomass is constituted of aromatic structures as suitable building blocks in many petroleum-based products, it emerges as a highly convenient and sustainable substitute in the production of materials [4]. As the impacts of extensive use of fossil-based products - including climate change, air and water pollution, ocean acidification, and reliance on non-renewable resources - have become apparent, it is increasingly clear that a shift towards more sustainable alternatives is not only desirable but imperative. One promising strategy to meet the demand for materials with characteristics similar to fossil-based products involves the adoption of bio-based materials derived from renewable resources like plants. This transition offers significant potential for mitigating the aforementioned environmental challenges while also promoting the development of a more sustain-

able and circular economy [5].

A technology with the primary goal of valorizing lignin, turning it into a valuable resource rather than treating it as a waste product, is the LignoBoost process, used to extract lignin from kraft pulp mill black liquor. The LignoBoost process was initially developed by Chalmers and RISE (former Innventia), but has been commercialized and further developed by Valmet. The world's largest plant for extraction of Kraft lignin was Stora Enso's Sunila Mill in Kotka, Finland before it closed in 2023. Using Valmet's LignoBoost process, the annual production capacity amounted to 50 000 tons [6].

Filtration is an important element of the LignoBoost process. Valmet has introduced a modification to the process by incorporating a thermal treatment on the lignin slurry in the final acidification phase before filtration [7]. Despite achieving a more efficient filtration, the challenge lies in the lack of understanding regarding the underlying reasons for the effectiveness of this heat-treating step. To gain insights into how the thermal treatment impacts the final filtration stage, a comprehensive study including characterization of the heat-treated lignin is required. By uncovering the structural and colloidal changes induced during the thermal treatment, Stora Enso and Valmet aim to optimize filtration properties and enhance the overall efficiency of the LignoBoost process.

1.1 Aim

The aim of this project is to gain an understanding of the reasons for improved filtration properties of the acidified lignin slurry following thermal treatment in terms of colloidal and structural changes. The focus includes investigating changes in the particle size distribution of treated lignin, analyzing variations in particle surface properties, exploring shifts in the molecular weight distribution of the treated lignin, and characterizing modifications in structural features, including linkages and functionalities. Ultimately, this would allow for tailoring of filtration properties and a more efficient process design. The main research question investigated is: what are the reasons for enhanced filtration properties of LignoBoost lignin with a thermal treatment of the acidified lignin slurry?

1.2 Limitations

In this work, some limitations have been set in order to define the project. Merely lignin that has undergone CO_2 precipitation has been used, and not black liquor. This ensures the lignin is equivalent to that used on industrial scale. Moreover, only a selection of conditions including temperature and treatment time has been analyzed; lignin has been thermally treated at 75°C, 85°C, and 95°C for 60 minutes. These have been established in consultation with Valmet and Stora Enso, and have been compared to a reference that has been processed at 55°C.

Two different sets of softwood lignin samples, *lignin A* and *lignin B*, were investigated in this project. The aim is not to compare them, but to find similar trends between the two. The differences between them arise from one being extracted in a pilot-scale equipment and the other in an industrial-scale mill, with varying mill conditions.

2
Theory

2.1 Lignin

Being one of the main components of the plant cell wall, lignin is the most abundant naturally occurring aromatic polymer, with the aromatic rings contributing to its rigidity. The structure of the lignin macromolecule is highly convoluted due to its heterogenous, three-dimensional, and randomly cross-linked matrix of three phenylpropanoid monomers called monolignols: *p*-coumaryl alcohol, coniferyl alcohol, and sinapyl alcohol [8], seen in Figure 2.1. The sole difference between the monolignols is the degree of methoxylation at the C3 and C5 positions of the aromatic ring. The complex matrix arises from a wide variety of linkages between the monolignols, contributing to the absence of repeated units [2].

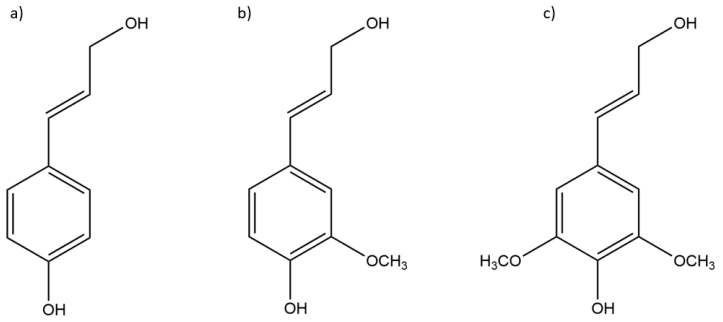

Figure 2.1: Molecular structure of a) *p*-coumaryl alcohol, b) coniferyl alcohol, and c) sinapyl alcohol.

The monolignols are precursor molecules in the biosynthesis of lignin, and are related to specific lignin units: *p*-coumaryl alcohol corresponds to *p*-hydroxyphenyl (H), coniferyl alcohol to guaiacyl (G), and sinapyl alcohol to syringyl (S). Lignin is biosynthesized through enzymatic dehydrogenation of the monolignols, which is a one-electron oxidation catalyzed by enzymes such as peroxidase or laccase. Radicals generated from a mix of monolignols within the cell wall react to form a dimer, subsequently undergoing radical coupling with either a monolignol, another dimer, or an oligomer. This sequence of radical couplings continues, leading to the formation of the lignin macromolecule [9].

The monomeric composition of lignin exhibits considerable variation across different species. In softwood trees, the primary constituents are G units, accompanied by

minor quantities of H units. In hardwood trees, the composition includes variable ratios of S and G units. In contrast, grasses and herbaceous materials display diverse ratios of H, S, and G units, contingent upon the specific plant species and tissue [10]. Softwood trees belong to a group called gymnosperms, and hardwood trees belong to angiosperms. The primary distinction between these lies in the manner in which their seeds undergo development. Angiosperms produce seeds within the ovaries of flowers, which are then enveloped by a protective fruit. On the other hand, gymnosperms typically generate seeds within unisexual cones, called strobili, and these plants lack both fruits and flowers [11]. Lignin contents range from 25–35% in softwood, 20–25% in hardwood, and 15–25% in herbaceous plants [12].

Native lignin refers to the unaltered lignin that is present within the cell walls of plants. The structure of lignin exhibits significant variability, depending on factors such as season, species, geographical location and even location within a plant [13]. Monolignols are connected by various interunit linkages, with the β-O-4 ether linkage being the most prevalent. This type of linkage constitutes about 45% of all interunit bonds in softwood native lignin. Other significant interunit linkages in lignin include the α-O-4 type, resinol (β-β'), phenylcoumaran (β-5), 5-5′, and 4-O-5 moieties. The abundance and distribution of these linkages can vary considerably among different types of lignin. The molecular structures of these are found in Figure 2.2 [14].

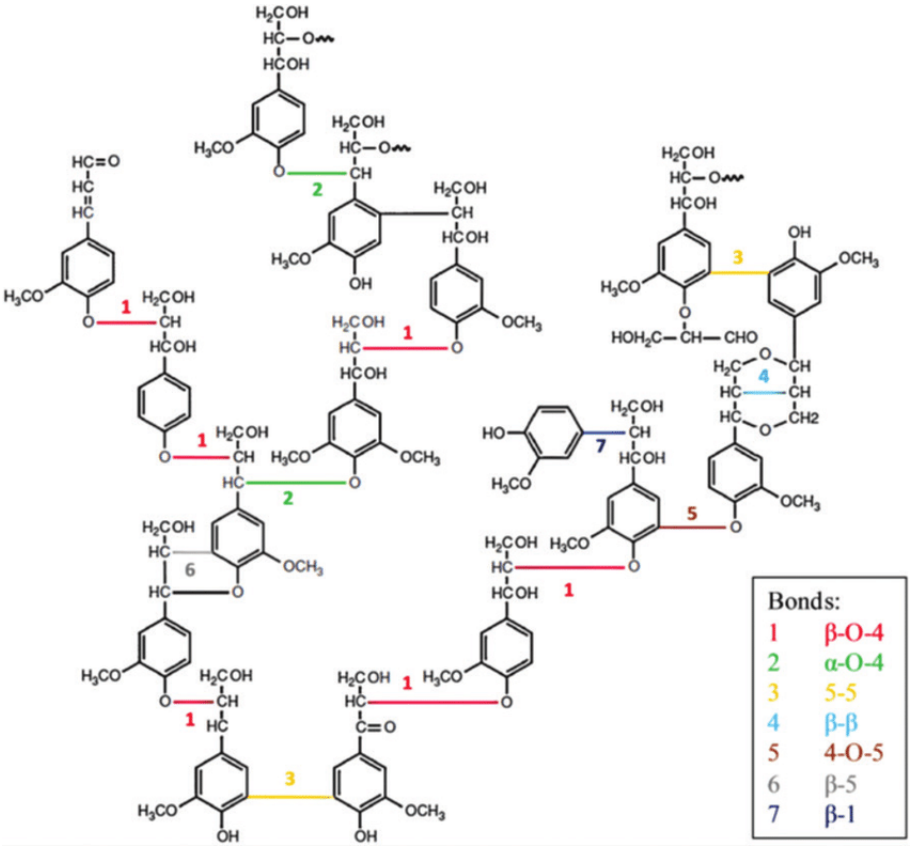

Figure 2.2: Main interunit linkages in softwood native lignin.

2.1.1 Technical lignin and valorization of lignin

The kraft process is a chemical process to produce wood pulp, which is the raw material used for production of paper, textiles, cellulose derivatives, etc. It uses a combination of sodium hydroxide and sodium sulfide called white liquor to fragment and solubilize lignin that binds the wood fibers together by cooking at elevated temperatures and pressures. The resulting mixture after the cooking is called brown stock, consisting of cellulose fiber and black liquor, the latter consisting of dissolved lignin, hemicellulose and chemicals.

During kraft pulping of wood, the structure of lignin is altered. This lignin - which has been extracted and processed from lignocellulosic biomass using an industrial method - is referred to as technical lignin, or in this case more specifically kraft lignin, and is different from native lignin. Softwood kraft lignin can be expected to be more uniform between different softwood species compared to hardwood, which is due to guaiacyl being the predominant building block [15].

Aryl-alkyl ethers, or β-O-4 bonds, are the main linkages in both softwood and hardwood lignin. During kraft pulping, most of these β-O-4 bonds are cleaved, yielding a large amount of phenolic compounds of lower molecular weight [16]. This results in kraft lignin having a lower molecular weight than the native lignin. Apart from the phenolic compounds, some carboxyl and aliphatic hydroxyl groups are also formed. With the change to lower molecular structures containing more phenolic groups, the lignin becomes more hydrophilic, which is also strongly promoted by the deprotonation of the phenolic groups in the highly alkaline solution, facilitating the separation from the rest of the lignocellulosic material [8].

Besides lignin, hemicelluloses are an ample constituent of wood, of which a small part can remain bound to lignin after kraft pulping. Softwood contains mostly two types of hemicelluloses: glucomannans, with the backbone consisting of D-glucose, and D-mannose units and xylan, consisting of D-xylose units [17]. Covalent bonds exist between hemicellulose and lignin, which likely influence the properties of the isolated lignin. During kraft pulping, xylan undergoes reactions which affects its structure and solubility. During cooking, it sustains alkaline hydolysis which cleaves some of the glycosidic bonds. It is also subjected to degradation during the peeling-off reaction by splitting off the reducing end groups of the carbohydrate chain. A previous study by Durruty et al. [8] have proved that xylan have a significant impact on the filtration properties of kraft lignin, as it increases the filtration resistance. One of the proposed explanations was that xylan is adsorbed on the surface of the lignin agglomerates and makes the lignin structure more porous locally, increasing the contact area between water and lignin. The sorbed xylan might also hinder the formation of a more dense filter cake which lowers the solidosity of the filter cake.

The perception of lignin has shifted from considering it a waste product to recognizing its potential as a valuable raw material. There are generally two approaches to valorizing lignin: one method involves utilizing lignin as a macro-polymer to create valuable materials, while the other method focuses on depolymerizing lignin

into low-molecular weight building blocks. To make use of lignin, it must first be separated from biomass through various processes, resulting in what is known as technical lignin. Since each method of lignin extraction alters its native structure differently, it is crucial to understand how these processes impact lignin structures in order to develop efficient lignin valorization technologies [18]. Table 2.1 lists some of the potential applications of lignin in several areas [8].

Table 2.1: Potential applications of lignin.

Fuel and syngas products	**Macromolecule-derived products**	**Hydrocarbons**	**Phenols**	**Oxidized products**
Methanol	Carbon fibres	Benzene	Phenol	Vanillin
DME	Polymer extenders	Toluene	Substituted phenols	B-keto adipate
Ethanol	Polyols	Xylene	Catechols	Vanillic acid
Fischer-Tropsch liquids	Thermoset resins	Cyclohexane	Resorcinols	DMSO
C1-C7 gases	Composites	Styrene	Eugenol	Aromatic acids
	Adhesives	Biphenyls	Syringols	Aliphatic acids
	Binders		Coniferols	Syringaldehyde
	Preservatives		Guaiacols	Aldehydes
	Pharmaceuticals			Quinones
				Cyclohexanol

2.2 The LignoBoost process

Different kinds of processes to extract kraft lignin from black liquor exist, such as Westvaco, LignoForce and LignoBoost, all of which are applicable on industrial scale, and sequential liquid-lignin recovery and purification (SLRP), which in the present is not applicable on industrial scale. All the processes use black liquor with 20-40% dry content of lignin as raw materia.

The extraction method of the lignin utilized in this project is based on the LignoBoost process. It involves two distinct steps: precipitation and washing. In the first step, lignin is separated from the mill's black liquor by lowering the pH using CO_2, causing lignin to precipitate. It is then separated from the black liquor with a press filter. In the second step, lignin is purified by washing, after additional acidification with sulfuric acid, in a low pH solution and then dewatered and further purified in a second filter press, yielding high purity lignin.

A schematic of the ordinary LignoBoost process, as well as the slightly modified one applied in this project is shown in Figure 2.3. The alkaline stage in the figure is the first step of the LignoBoost process and the acidic stage is the second step where the lignin is purified in a low pH solution. The intermediate steps are the

separation steps by dead-end filtration. The difference between them is the order of the thermal treatment and filtration toward the end of the extraction. Recently, a thermal treatment of the lignin at 85°C was introduced which resulted in improved filtration. For practical reasons the experimental work conducted for this master's thesis was done on lignin that had already been acidified and washed. Preparing acidified and heat-treated lignin from black liquor or alkaline stage lignin would have added considerable time to the experimental work.

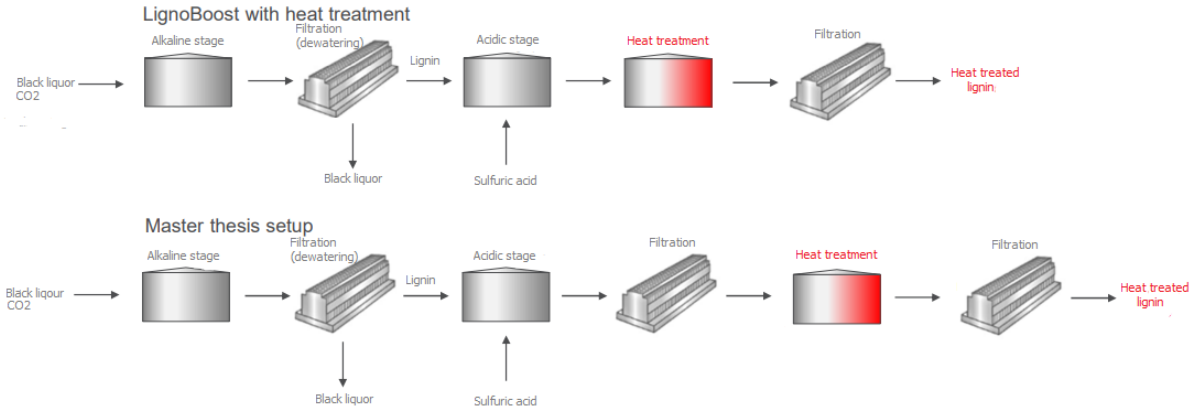

Figure 2.3: Schematic of the ordinary LignoBoost process and the modified version used in this project.

2.3 Thermal treatment of lignin

It is well-established that subjecting lignin to elevated temperatures induces alterations in its chemical composition and inherent properties. This phenomenon has been recognized in numerous prior studies [19, 20, 21]. However, no studies investigating thermal treatments in similar settings regarding temperature range and slurry conditions were identified in the existing literature, and neither were any related to filtration properties. The lowest thermal treatment temperature found in literature was 100°C, and no investigated lignins were suspended in a slurry during thermal treatment; rather, they were either dried or subjected to heat while being in its native state in the source plant.

One demonstration of thermal treatment applied to a lignocellulosic material was showcased by Brosse et al. [19], who treated beech wood at 230°C for 7 h, and compared Klason lignin and milled wood lignin extracted under acidic conditions before and after treatment. An extensive cleavage of α- and β-aryl-ether linkages was ascribed to the decrease in intensity of the NMR signals assigned to the carbon atoms of the lateral chain (C_α,C_β and C_γ). Moreover, reduced amounts of protonated aromatic carbons (Ar-H) and elevated levels of condensed aromatic carbons per aromatic ring (Ar-C) translate to a more condensed structure. This suggests that hydrolytic cleavage and polymerization by condensation occur concurrently, at least at 230°C. Overall, the average molecular weight decreased, indicating that thermal treatment degraded the macromolecular structure of lignin.

To reach a more comprehensive understanding of how lignin is affected by heat, Kim et al. [20] exposed hardwood samples of milled wood lignins isolated under acidic conditions according to the Bjorkman method, to temperatures between 150 and 300°C with an increase of 50°C, for 10 minutes each. Coupled to a GC-MS system, 26 compounds of monomeric phenols of four different types (C_6C_3, C_6C_2, C_6C_1, and C_6) were identified. However, none of these were visible below 250°C, at which they were in very low amounts compared to at 300°C. This trend likely occurs as a result of there being an increased breakdown of terminal phenolic groups, attached by thermally labile β-O-4 linkages within the lignin polymer, as volatile compounds evaporate during thermal treatment. This corresponds well to research conducted by Nge et al. [21] on softwood-derived glycol lignins, where Klason lignin analysis showed no apparent degradation at temperatures up to 220°C, with treatment duration of 1 h.

Further, observed as a general pattern among heat-treated lignins is that thermal gravimetric analysis (TGA) results showed a positive correlation between treatment temperature and thermal stability, with onsets of this enhanced stability at treatment temperatures between 140 and 160°C [20, 21].

A contrasting trend to the studies mentioned above regarding molecular weight was observed by Wojtasz et al. [22, 23]. In their experiments, lignin from birch and spruce was extracted using hot water extraction under acidic conditions and in the temperature range more relevant for this work (130-170°C). In both cases, the molecular weight was observed to increase with elevated temperature and treatment time, suggesting that the aqueous medium, or lack thereof, as well as temperature range are of great importance for how the molecular weight of lignin is changed during thermal treatment.

It should be emphasized that structural and hence physical properties of lignin are altogether dependent on origin and extraction method, meaning results from corresponding measurements can vary significantly between different types of lignin.

2.4 Filtration of kraft lignin

Filtration stands as a pivotal unit process across numerous industries, facilitating the segregation of liquids and solids. This function serves various purposes, such as isolating the reaction medium from the product and achieving purification [24].

Dead-end filtration operates by subjecting the suspension to a pressure gradient, allowing only the liquid and particles smaller than the pore diameter to permeate through a filter medium. This results in the gradual formation of a filter cake as liquid is extracted. Separation demands that the pressure difference across the filter cake exceeds the resistance of both the filter medium and said cake. The resistance of the filter cake originates from the frictional and form drag forces experienced during the flow of liquid through interstitial space between the solid particles [24].

Materials have different filtration properties, and the filterability of a component depends mainly on two factors: cake solidosity, which characterizes the solid content of the filter cake, meaning the volume-based proportion of solids within it, and filtration resistance, meaning the pressure drop across a filter at a stated flow and under given conditions. Enhanced filterability is associated with increased solidosity and decreased filtration resistance. These properties are, in turn, influenced by factors such as particle size and shape, as well as the mechanisms of particle-particle/slurry interactions that operate during the cake build-up stage, such as friction, interlocking between particles, electrostatic forces and van der Waals forces. These factors affect the solid structure of the filter cake, hence influencing its filtration properties [8]. Other factors such as particle size distribution, porosity, surface characteristics, molecular weight distribution, and molecular structure may also have an impact on filtration properties.

The two main forces that act between particles themselves, as well as between particles and the liquid medium, are attractive van der Waals forces and repulsive electrostatic forces. When discussing the impact of charge and electrostatic forces, it is crucial to differentiate between surface charges and bulk charges. Charged colloidal particles dispersed in an electrolyte solution attract ions of opposite charge, which form an electrical double layer. These regions are known as the Stern layer, a thin layer of immobile counterions closest to the charged surface, and the diffusive layer, an ionic cloud close to the surface where the concentration of counterions is higher relative to coions. In effect, the net repulsive force between particles is represented by the ζ potential [25].

A study conducted using model particles, consisting of a polystyrene core with varying ratios of charged and uncharged stabilizing polymers covalently attached to the surface, revealed that both porosity and specific filtration resistance increased with particle charge. Typically, higher porosity would lead to lower filtration resistance; however, this study demonstrated that the influence of surface charge surpasses that of porosity. Existing models even failed to predict the specific cake resistances of highly charged filter cakes, as these cakes exhibited resistance levels orders of magnitude higher than expected. Deviations from traditional behavior, likely stemming from the confinement of charged particles by charged walls or pores, offer a potential explanation. This scenario permits the interpretation of elevated resistances as resulting from increased osmotic pressure due to the dispersion of counterions in the pores [26]. While a ζ potential closer to 0 mV yields more rapid filter cake formation and higher filtration rate, the moisture content of the filter cake is generally higher. This result is attributed to particle aggregation within the suspension when interparticle repulsion forces are diminished [27].

Separation behavior can also be altered by controlling the concentration of non-adsorbing electrolytes in the liquid medium to change the distribution of solution ions around the particle. With increasing ionic strength of the bulk, the diffusive layer attenuates due to an increasing concentration of counterions, thus causing the

surface charges to become shielded. This weakens the repulsive electrostatic forces. If the potential energy of the repulsive forces is reduced to the point where the attractive van der Waals forces dominate, particle agglomeration is promoted, making the dispersion more easily separated [28].

The effect of interactions between a particle and the liquid medium in which it is suspended is most significant when the particle size is smaller than around 10 µm. Nevertheless, particle size influences filtration properties in additional manners. In practical terms, feeds are rarely composed of monosized particles; instead, they typically encompass a distribution of sizes. Regarding filtration properties, it is the smallest fraction of the size distribution that present the greatest contribution. These particles are small enough to migrate through the interstitial spaces of larger particles in the flow direction and concentrate in the cake layers closest to the filter. Since bodies of a given shape have a higher surface area to volume ratio with decreasing size, smaller particles have the biggest impact on the specific surface area [27]. Larger specific surface area being subjected to the flow of the liquid medium implicates higher frictional drag forces and therefore, higher filtration resistance [24]. Small particles can occupy interstitial spaces between larger ones, thus decreasing cake porosity, which positively correlates to the permeability of a material [29]. However, porosity is not determined by particle size. Rather, it depends on the distribution of particle sizes; a broader size range allows particles to pack more densely [27].

Further, particle shape is also a determining factor for filtration efficiency, as it governs its specific surface, S_0, defined as the surface area divided by volume. It is worth noting that solid particles are rarely regular in shape or uniform in the distribution of shapes. Instead, suspensions are oftentimes comprised of a range of shapes, with varieties in surface roughness, surface chemistry and porosity, to mention a few [30]. However, general trends in said range can be related to the specific resistance of the filter cake. Figure 2.4 demonstrates how common particle shapes affect the specific surface. For cylindrical particles, two cases can emerge depending on the length to diameter ratio. If $a >> b$, the particle is fibrous, and yields a low specific surface, while if $a << b$ the particle is flaky and yield a high specific surface. The specific resistance α of the filter cake is proportional to the square of the specific surface [27].

	Shape	Surface	Volume	Specific surface
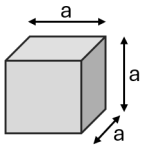	Cubic	$6a^2$	a^3	$\frac{6}{a}$
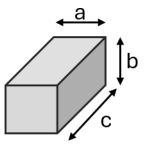	Rectangular	$2(ab + ac + bc)$	abc	$\frac{2(ab + ac + bc)}{abc}$
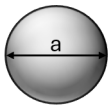	Spherical	πa^2	$\frac{\pi a^3}{6}$	$\frac{6}{a}$
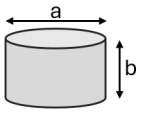	Cylindrical	$\frac{\pi a^2}{4} + \pi ab$	$\frac{\pi a^2 b}{4}$	$\frac{4}{a} + \frac{1}{b}$

Figure 2.4: Effect of particle shape on specific surface.

3
Methodology

To evaluate different aspects affecting the filtration properties of LignoBoost softwood kraft lignin, different analytical measurements and performance measurements were utilized.

3.1 Thermal treatment and filtration

LignoBoost softwood kraft lignin with a dry content of 42.9%, lignin A, and LignoBoost softwood kraft lignin with a dry content of 63.2%, lignin B, were received from Stora Enso. The received lignin had been filtrated prior to treatment, in contrast to the industrial process where the lignin is filtrated after treatment. Lignin A was suspended in 100 g H_2SO_4 pre-acidified tap water at pH 2.5 to make a 20 weight% lignin suspension. Lignin B was suspended to the same weight% with 80 g pre-acidified tap water. The pH was measured and adjusted to 2.5 with H_2SO_4. The suspension was left to stir with a propeller magnet for 60 min. The suspension was then transferred to a 500 mL round bottom flask in an oil bath with a magnetic stirrer. Attached to the round bottom flask was a condenser and a temperature probe. The suspension was heated up to 55°C and let stabilized for 5 min under 1000 RPM stirring. It was then adjusted to the desired temperature of 55, 75, 85, or 95°C and treated for 60 min. After thermal treatment the suspension was cooled down to 60°C in a water bath and was poured into a 7 cm vacuum filter and filtrated for seven min. The time was noted when the top of the filter cake dried. The dry content of the lignin was measured before and after treatment with a moisture analyzer at 160°C. For lignin A, three replicates per treatment temperature were made while for lignin B, only one per treatment temperature was made due to shortages in the supplied material.

Before every measurement performed with lignin slurry, the slurry was either shaken thoroughly or vortexed to disrupt phase separation. For every measurement with lignin powder the samples were either dried in an oven at 50°C or vacuum-dried to achieve >95% dry content. Most of the measurements were performed on two different varieties of lignin samples, A and B. Note that the concentration of the slurries were the same but the volume when heat treating lignin B was lower than when heat treating lignin A. A flowchart of the methodical process can be seen in Figure 3.1.

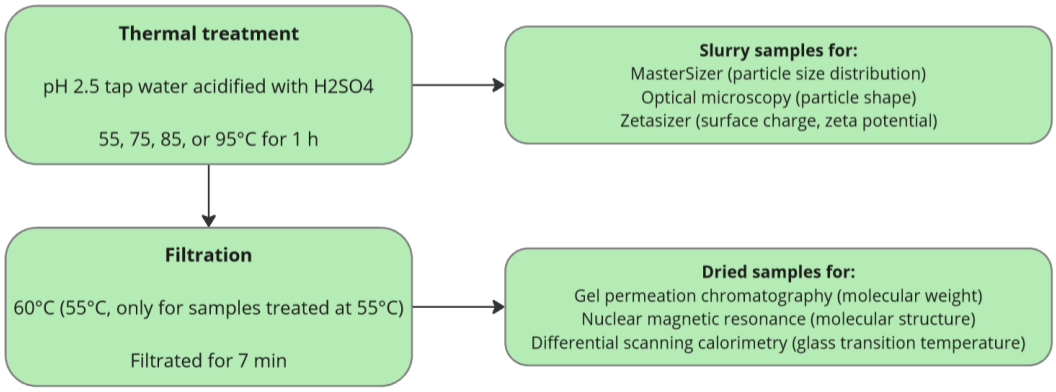

Figure 3.1: A simplified overview of the methodical process, also illustrating the types of samples used for various analysis methods.

3.1.1 Yield measurement

A solid yield test was conducted, where the filter cake was weighed after filtration with samples that had been heat-treated at all mentioned temperatures for 15 min, and one sample at 85°C for 60 min.

Filtrate from samples that had been heat-treated for 60 min was collected. The filtrate was then analyzed by UV-Vis from 700 to 200 nm to observe if any lignin was transferred to the filtrate during the filtration.

3.2 Colloidal properties

3.2.1 Particle size distribution (PSD) analysis

To measure the particle size distribution of the treated lignin (PSD), a Mastersizer 2000 with a Hydro 2000s module attached from Malvern Industries was utilized, based on laser diffraction with a detection range between 0.02 and 2000 µm. Samples were extracted directly from lignin slurry during heat treatment and mixed with deionized water after it had reach its desired temperature and been treated for 0, 15, 30, 45, or 60 min. The samples were then inserted into the Hydro 2000s until the obstruction of the laser was between 9-10%. RPM for the mixer was set to 1750 and ultrasound to 100%. The refractive index of lignin was set to 1.61.

3.2.2 Optical microscopy

Optical microscopy analysis was conducted to confirm the results seen with PSD and to observe changes in the particle shape. 20 µL of lignin slurry was diluted with 2 mL pH 2.5 H_2SO_4. 20 µL of the diluted sample was mounted onto a glass slide to be optically analyzed with a Zeiss Discovery V.12, using a Zeiss KL1500 LCD as a light source. The magnification used was 230x for all samples.

3.2.3 ζ potential

The ζ potential was analyzed to understand how the surface charge affects the colloidal properties in terms of agglomeration behavior, as well as connecting this to the filtration properties of the lignin. Slurry samples were extracted after 60 min of heat treatment and were diluted 4000 times. The samples were then transferred to a disposable ζ potential cuvette and analyzed with a Malvern Zetasizer Ultra.

3.3 Structural properties

3.3.1 Gel permeation chromatography (GPC)

Gel permeation chromatography (GPC) was used to determine the molecular weight distribution of the samples. 10 mg of dried lignin sample was dissolved in 1 mL of DMSO containing 10 mM LiBr. The solution was vortexed and left to fully dissolve for 24 hours. 100 µL of the solution was diluted with a filter syringe into a 4 mL vial with 10 mM LiBr DMSO. The molecular weight distribution was measured with UV and refraction index detection. The GPC instrument used was a PL-GPC 50 from Polymer Laboratories, attached with a Polargel-M Guard 50*7.5 mm guard column and two 300*7.5 mm PolarGel-M columns.

3.3.2 Nuclear magnetic resonance (NMR)

Both ^{13}C NMR and heteronuclear single quantum coherence (HSQC) ^{1}H ^{13}C 2D NMR were performed on lignin A to investigate whether there were any structural changes affecting the filtration after heat treatment affecting the filtration properties. Samples for ^{13}C NMR were prepared by dissolving 150 mg of lignin sample in 1 mL of d6 DMSO with 3 mg of Cr(III) acetylacetonate and 10-15 mg of 1,3,5-trioxane working as an internal standard. Samples for HSQC NMR were prepared by dissolving 50 mg of lignin in 500 µL DMSO. HSQC integration was performed according to a study by Lancfield et al. [31].

3.3.2.1 Acetylation for NMR characterization

For improved complementary NMR analysis, the lignin samples were peracetylated according to the following procedure. 300 mg of lignin was added with 9 mL of acetic anhydride and 9 mL of pyridine in an Erlenmeyer flask to stir for 24 hours. The sample was then added to 200 mL of 0.01 M HCl (aq), and filtered using a vacuum filtration. It was rinsed once with 200 mL of 0.01 M HCl and three times with deionized water. The resulting filter cake was oven-dried at 50°C for 4 days. The dried samples were prepared the same way as the non-acetylated ^{13}C NMR samples described in Section 3.3.2. Calculations to quantify specific structures with the help of acetylation were performed according to a study by Balakshin et al. [32].

3.4 Thermal properties

3.4.1 Differential scanning calorimetry (DSC)

Differential scanning calorimetry (DSC) analysis was carried out on both lignin A and B to provide complementary information about occured chemical reactions and aid in understanding the NMR results. Moreover, it allowed for the examination of the glass transition temperature (T_g) of the samples, which can be affected by the amount of crosslinking of the molecules. Samples were weighed between 2 to 5 mg into a hermetic aluminum sample pan. The DSC had a N_2 gas flow of 50 mL/min. The temperature at the start was 25°C, then increased to 220°C and then decreased to 0 °C at a rate of 10°C min^{-1}. This cycle was then repeated one more time. The DSC instrument utilized was a Mettler Toledo DSC5+.

4

Results and discussion

4.1 Thermal treatment and filtration

Thermal treatment was performed at four different temperatures, 55, 75 85, and 95°C, each for the two different varieties of lignin. For both lignin A and lignin B, the filtration time decreased with increasing temperature between 55 to 85°C, and then an increase in filtration time for the thermal treatment performed at 95°C, relative to treatment at 85°C. This change in filtration time can be observed in Table 4.1. However, the dry content of the filter cake was observed to increase with increased temperature, with a drastic change between 85 and 95°C.

Table 4.1: Filtration time and dry content for the different thermal treatments of lignin A.

Temperature (°C)	**Filtration time (s)**	**Average (s)**	**Dry content (%)**	**Average (%)**
55	330		37.90	
55	360	403.3	35.46	37.42
55	520		39.10	
75	60		44.07	
75	60	56.7	44.47	44.07
75	50		43.68	
85	27		45.40	
85	30	31.0	45.83	45.50
85	36		45.26	
95	70		58.30	
95	100	77.7	60.30	60.50
95	63		62.89	

The same trends found for lignin A in Table 4.1 can also be seen for lignin B, although it was sourced from slightly different process conditions in Table 4.2. The filtration time decreased to 85°C and then increased again for 95°C and the dry content increased with increasing temperature.

Table 4.2: Filtration time and dry content for the different thermal treatments of one replicate of lignin B.

Temperature (°C)	Filtration time (s)	Dry content (%)
55	50	46.49
75	24	46.06
85	8	67.23
95	13	72.76

The filtration time was lower for 95°C than for 75°C for lignin B, this could however be because of error in measurement of the filtration. The observed changes in filtration time and dry content with increased temperature for lignin A and B suggest that the lignin undergoes transformation during the treatment. This will be explained in more detail with the forthcoming results.

4.1.1 Filtration yields after the thermal treatment

Gravimetric yield measurements in filter cakes and UV-Vis of the filtrates were conducted at all heat treatment temperatures after 15 min of treatment and filtration, including one measurement after 60 minutes of treatment. Measured solid yield can be observed in Table 4.3, and can be seen to have decreased with increased temperature. Before making these slurries for these samples, it was noted that mold had started to form. It is unclear whether if and how this affects the results.

Table 4.3: Yield measurement of lignin A after thermal treatment.

Temperature (°C)	Solid yield (%)
55	97.7
75	91.5
85	86.7
95	81.3
85 (60min)	89.2

Indeed UV-Vis measurements of the filtrates could confirm increased dissolution of lignin structures with the increasing treatment temperature as can be seen in figure 4.1.The peak of interest is located around 275 nm, which is related to the absorption of aromatic units. From Figure 4.1 it is evident that the amount of UV-absorbing structures released to the liquid phase increases with the treatment temperature, thus confirming the results from the solid yield measurements. This is likely explained by the cleavage of certain bonds followed by dissolution of these cleaved structures, or by increased dissolution of existing lignin structures, or most likely a combination of both. The fact that the solid yield is decreasing with increased temperature can probably be attributed to increased solubility of the treated lignin promoted possibly by decrease in molecular weight by linkage cleavage.

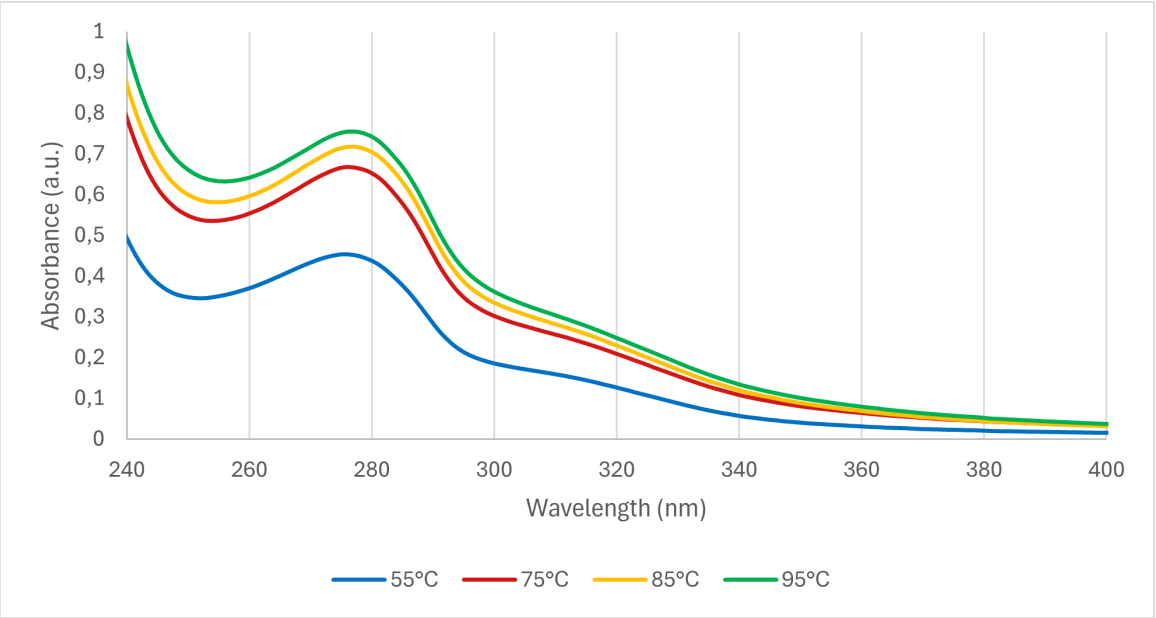

Figure 4.1: UV-Vis spectra of the liquid filtrate from lignin A heat treatments.

4.2 Colloidal properties

In this section, results from an in-depth analysis of the colloidal properties of lignin particles are presented and related to filtration properties, focusing on particle size distribution, particle shape, and surface charge.

4.2.1 Particle size and shape

Initially, focused beam reflectance measurement (FBRM) was intended to be used for determining the chord length distribution as it would allow for *in situ* real-time monitoring. Unfortunately, it was observed to generate inconsistent results. Numerous attempts were made to find the cause of and eliminate the errors. These attempts included measuring suspensions of 1 weight% lignin to check if the high concentration was causing the problem, and cleaning the probe window between measurements as lignin was seen to adsorb to it. During these trials, the FBRM instrument achieved equivalent particle counts in 20 weight% lignin suspensions as in 1 weight% ones, as well as giving off signal when probing air. Therefore, FBRM was discontinued.

Subsequent to discovering the incompatibility with the FBRM instrumentation, the Malvern MasterSizer 2000 with a Hydro 2000s module was chosen instead as a means of measuring the particle size distribution (PSD). Although, this implied that the chronal resolution was heavily compromised as it shifted from virtually real-time to 15 min. While this is a drawback of the MasterSizer, it instead allows for obtaining quantitative results of both the number- and volume-based size distribution information of the particles. By considering both of these, a more comprehensive understanding of the particle size distribution is gained. Number-based size dis-

tribution emphasizes the particle count distribution, indicating the prevalence of different particle sizes in terms of count. This aids in understanding the connection to filtration, as this hinges on the significance of smaller particles, which, due to their elevated surface-to-volume ratio, exert the greatest influence on filtration resistance. However, if there are a few particles that account for a large volume, this fraction may not be resolved by the number-based size distribution. This will be addressed by the volume-based size, reflecting the contribution of each particle size to the total volume of the sample, as well as agglomeration tendencies.

Displayed in Figures 4.2 and 4.3 are the PSDs of lignins A and B with respect to the number percentage. It is evident that treatment temperatures up to 75°C do not impact the particle size to a degree where it could account for the dramatic differences in filtration properties. Hence, there must be another parameter that is changed during the thermal treatment which explains the improvement in filtration efficiency between 55 and 75°C for both lignins A and B, as observed in Tables 4.1 and 4.2. Above 75°C, the PSDs shift toward larger particles with increasing temperature. Except for lignin B treated at 95°C, the majority of particles are below 10 µm in size, the range in which the effect of interactions between particles and the liquid medium is most significant. Above this size is where gravitational forces tend to dominate. Therefore, it could be assumed that the effect of the ζ potential on filtration properties will be non-neglible.

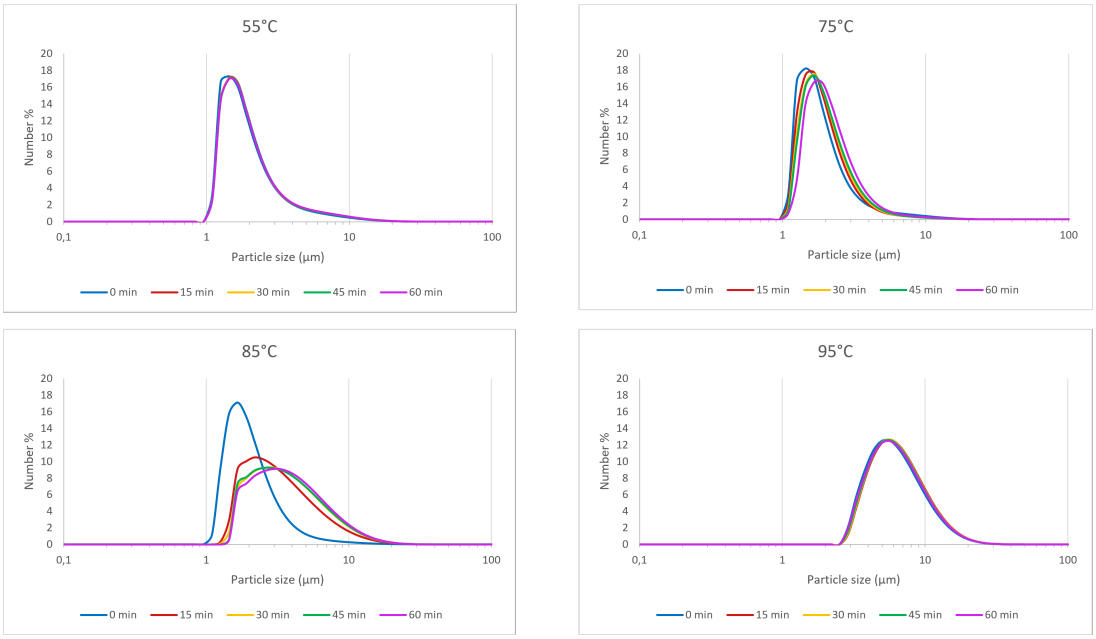

Figure 4.2: Particle size distributions of lignin A based on number particle count.

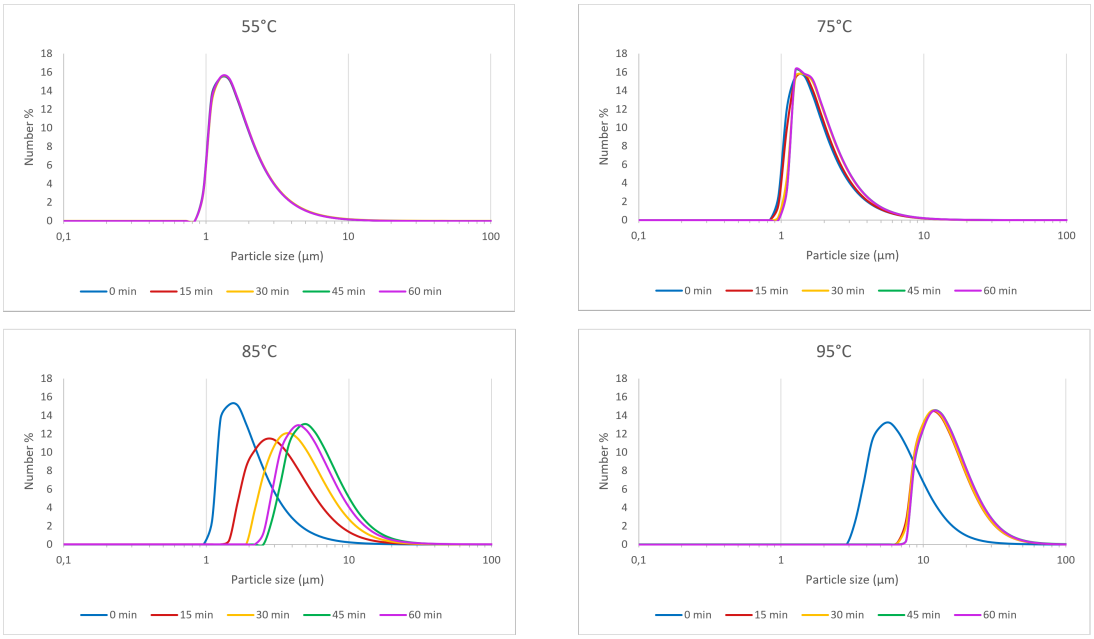

Figure 4.3: Particle size distributions of lignin B based on number particle count.

Many of the same trends are, as could be expected, found when considering PSDs measured as volume percentages, as shown in Figures 4.4 and 4.5. Worth noting is the rise of the shoulder peak in the 75°C treatment of lignin A as time progresses, which is seen to disappear after 15 min in the 85°C treatment. It is yet unclear why this peak emerges, but it could possibly be explained by varying rates of depolymerization and crosslinking reactions, as will be discussed later in this report. Examining the volume percentage for the 75°C it seems that the average particle size decreases during the first 45 min of treatment, and then increasing again between 45 and 60 min. However, the number percentage discloses a continuous increment in particle size. During thermal treatment, two physical processes also play significant roles: dissolution and agglomeration of particles. These processes are likely to dominate at different temperature and time intervals, potentially in conjunction with chemical reactions such as depolymerization or crosslinking. Dissolution might for instance be related to depolymerization as this can result in smaller lignin molecules that are more easily dissolved. On the other hand, agglomeration involves the clumping together of particles, which may become more prominent at higher temperatures or later stages, possibly as a result of the increased mobility and collision frequency of particles. Moreover, the volume percentages reveal that most of the volume is occupied by particles larger than 10 µm in size, with many of these not being accounted for by the number percentage to any extent.

Although the PSDs measured as number percentage were similar between lignin A and B, Figures 4.4 and 4.5 highlight the differences in size between them, arising from different mill conditions during extraction, resulting in two distinct lignins. The most substantial change in PSD for both varieties of lignin is observed around 85°C. However lignin A begins to show significant alterations already at 75°C, indicating that the thermal response of lignin varies depending on its type, with lignin A being

more sensitive to heat at lower temperatures compared to lignin B.

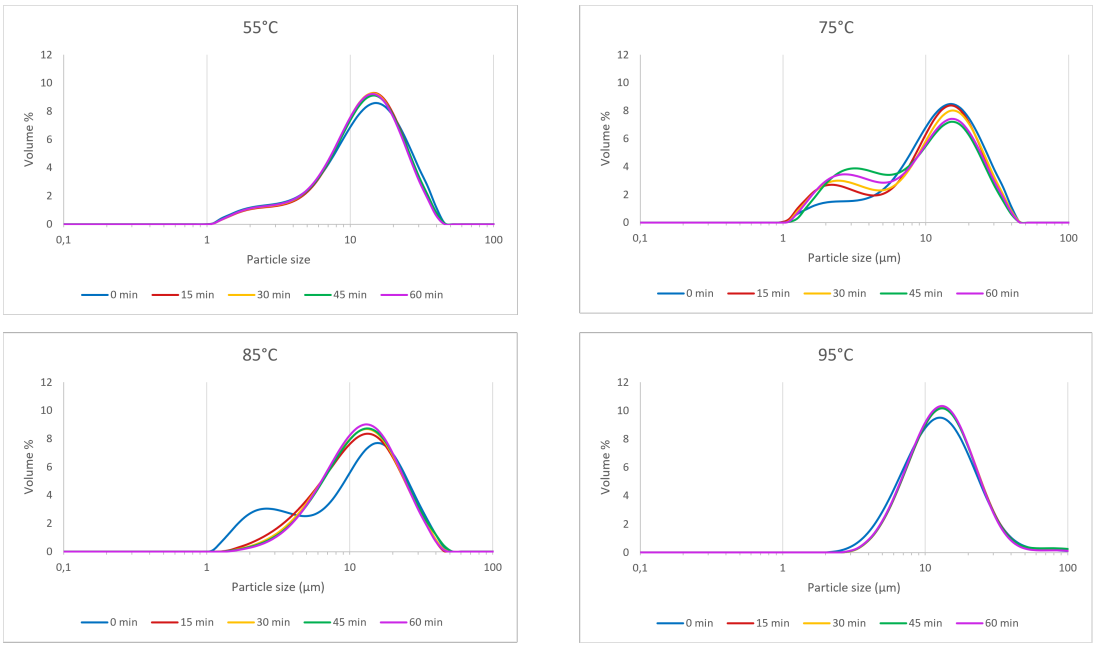

Figure 4.4: Particle size distributions of lignin A measured as the volume percentage.

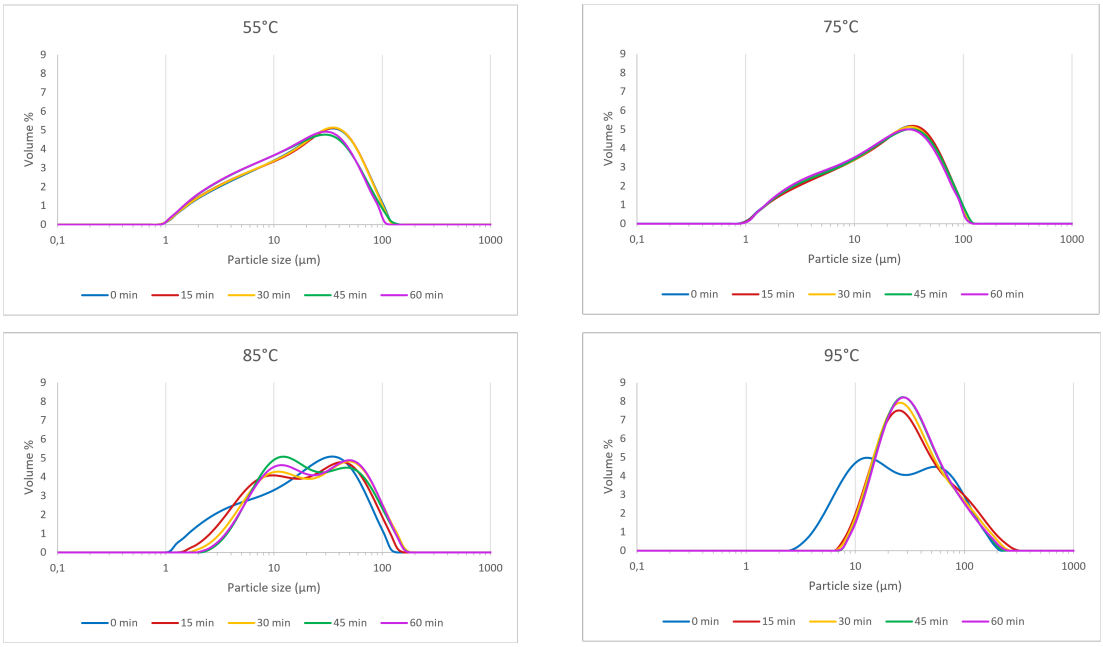

Figure 4.5: Particle size distributions of lignin B measured as the volume percentage.

The number and volume percentages in combination aid in uncovering the dispersity in the distribution of particle size, which contributes to the porosity of the filter cake. Noting that Figures 4.2 – 4.5 are in logarithmic scale, it is observed that the

broadness of the curves increase with increased temperature. This implies that filter cakes formed from slurries treated at higher temperatures would be able to pack more densely and thus exert a higher resistance to filtration, although the average particle size for those is larger. This is related to porosity and its dependence of broadness of the distribution rather than the particle size, as described in Section 2.4, analogous to a container filled with a mixture of large marbles and small beads. If only large marbles are present, they will leave significant gaps between them, resulting in a loosely packed container with plenty of empty space. This represents a system containing relatively large particles with a narrow particle size distribution. Now, if small beads are added to the container, these beads will fill the gaps between the marbles, allowing for a much tighter packing. The smaller beads occupy the spaces that the larger marbles cannot fill, which reduces the overall void space and increases the packing density of the mixture. This analogy illustrates why porosity is independent of the average particle size but is strongly influenced by the particle size distribution. When the particle size range is wider, the mixture of large and small particles can pack together more efficiently, similar to how small beads can fill the gaps between large marbles, resulting in a denser and less porous structure. Therefore, a wider size distribution allows particles to pack more tightly, reducing the overall porosity of the material. Despite the supposed reduced porosity of the filter cakes, these slurries filter more easily. Consequently, beyond providing indirect clues, it is not possible to accurately determine the filter cake porosity from these results and prove that porosity does not have a significant impact on filtration.

One of the fundamental aspects of particle characterization involves observing their shape and morphology. Microscopic analysis provides direct evidence of the size and shape of the lignin particles, enabling elucidation of their structural features at the microscale, which are tightly correlated with the filtration properties of the lignin slurry. The rationale behind adopting microscopic analysis for this inquiry stems from the fact that all recorded particles were within the detection range of optical microscopy. Additionally, since the samples were not dry, they were not suitable for electron microscopy as this technique operates under high vacuum.

Images of lignin A and B slurries treated at different temperatures are shown in Figures 4.6 and 4.7, respectively. From these images, it is possible to deduce that the particles are to some extent spherical, but mostly irregular in shape. Of greater significance is that they do not change in shape with increasing treatment temperature, meaning it can be concluded that particle shape does not explain why filtration properties improve by thermal treatment. Yet, these images visually verify the pattern previously seen in the PSD results; particles shift to larger sizes with increasing treatment temperature, both regarding number and volume percentage. This shift is most distinctive between 75 and 85°, corresponding to b) and c) in Figures 4.6 and 4.7, where the smallest fraction of particles seem to have vanished.

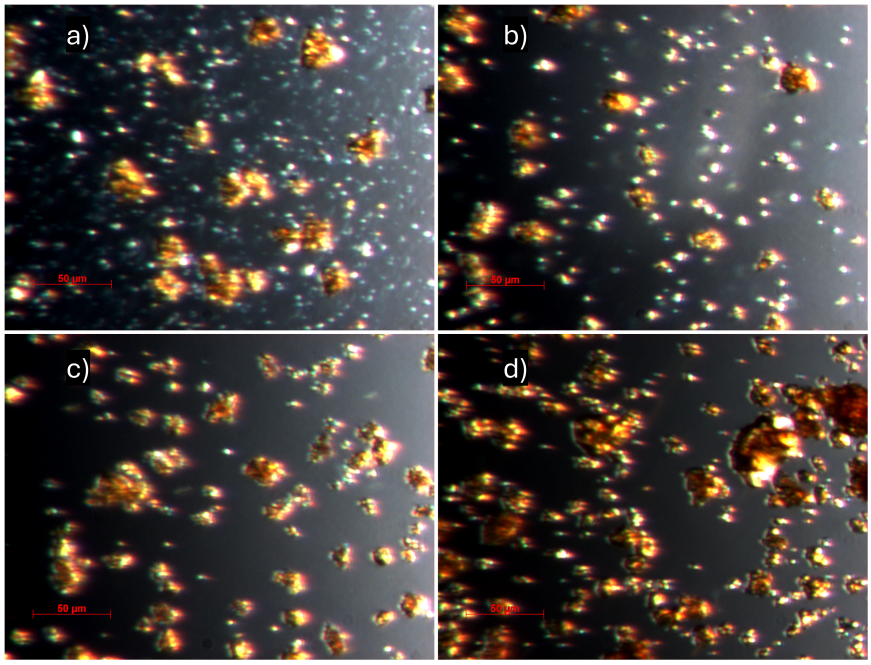

Figure 4.6: Microscopy images of lignin A slurries treated at a) 55°C, b) 75°C, c) 85°C and d) 95°C, at 230x magnification.

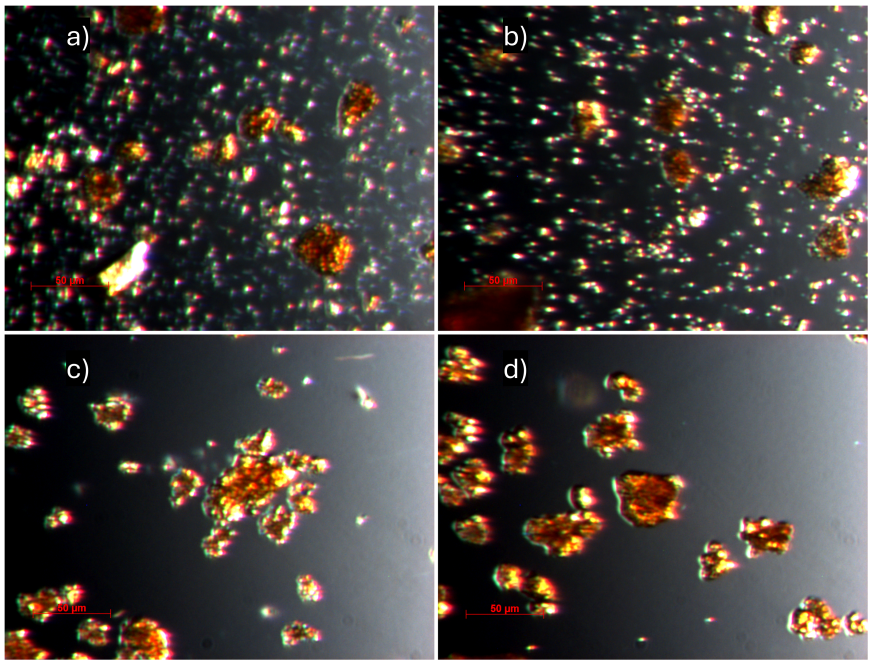

Figure 4.7: Microscopy images of lignin B slurries treated at a) 55°C, b) 75°C, c) 85°C and d) 95°C, at 230x magnification.

4.2.2 Surface charge

Thermal treatment of lignin suspended as particles can break and form bonds within the lignin structure, ultimately altering the surface chemistry and possibly also the

surface charge of the particles, which is closely interconnected with the ζ potential. Decreasing the strength of the repulsive forces, closely associated to the ζ potential, leads to instability in the dispersion, making the slurries more easily separated by filtration.

Initially, the LignoBoost lignin typically exhibits negative ζ potential due to the presence of the anionic functionalities. From Table 4.4, it is obvious that the ζ potential approaches zero with increasing treatment temperature. Both lignins A and B indicate a drastic drop between 75 and 85°C, which could possibly explain the difference in filtration properties between those. However, they do not conform with theory predicting that the dry content of the filter cake should be lower with more neutral ζ potentials. That is under the assumption that all other parameters stay constant, which is obviously not true for this particular case. For instance, the thermal treatment led also to a broader particle size distribution, as discussed above.

The trend of increasing ζ potential implies that particles treated at higher temperatures are more prone to agglomeration, which is reflected by the shift toward larger particle sizes in Section 4.2.1, commencing between 75 and 85 °C. The altered agglomeration behavior may be due to the significant drop in surface charge potential between the two treatment temperatures, which reduces electrostatic repulsion and promotes particle agglomeration, resulting in increased particle size. The exact cause of this change in surface charge is unclear, but it is likely linked to chemical reactions occurring above 75°C that modify the particle surface chemistry by reducing the number of charged groups.

Table 4.4: ζ potentials for lignins A and B at different treatment temperatures. Values are averages from 12 measurements on one replicate per sample.

Sample	**ζ potential (mV)**
55A	-16.2
75A	-15.5
85A	-10.0
95A	-8.6
55B	-17.1
75B	-15.1
85B	-7.9
95B	-6.0

It should be noted that all measured values are relatively low. In literature, colloidal dispersion with ζ potentials below ± 30 mV are considered unstable. From ± 10 to ± 30 mV, the stability behavior is classified as incipient instability, and below ± 10 mV indicates rapid coagulation or flocculation [33].

4.3 Structural properties

Structural properties relate to the chemistry of the individual lignin macromolecule, which comprises a number of different linkages and functionalities and as such influence both size, morphology and surface properties of the particles. Analysis was made with regards to molecular weight distribution and molecular structure.

4.3.1 Molecular weight distribution

GPC measurements can be used to observe the extent of depolymerization and polymerization or cross-linking of lignin. The GPC results shows an increase in molecular weight with increased treatment temperature, as shown in Table 4.5.

Table 4.5: GPC results for lignin A, with weight average molecular weight (M_w), number average molecular weight (M_n) and the polydispersity index (PDI).

Temperature (°C)	**M_w (Da)**	**M_n (Da)**	**PDI (M_w/M_n)**
55	9086	1339	6.79
75	9376	1347	6.96
85	9850	1362	7.23
95	10738	1422	7.55

Most of the changes in M_w occur between 2000 and 100 000 Da, meaning molecules below 2000 Da seem to not react significantly, as seen in the chromatogram presented in Figure 4.8. Guaiacyl, the primary monolignol in softwood lignin, has a M_w of around 180 Da. This indicates that the lignin molecules that are most affected by the heat treatment has at least 10-12 linkages. There are some, but very few, changes in the molecular weight distribution occurring during the treatment. Because of this, it can be concluded that the cause behind the change in filtration is possibly not strongly related to changes in molecular weight, even though a modest but consistent shift towards higher molecular weights has been observed when the treatment temperature was increased.

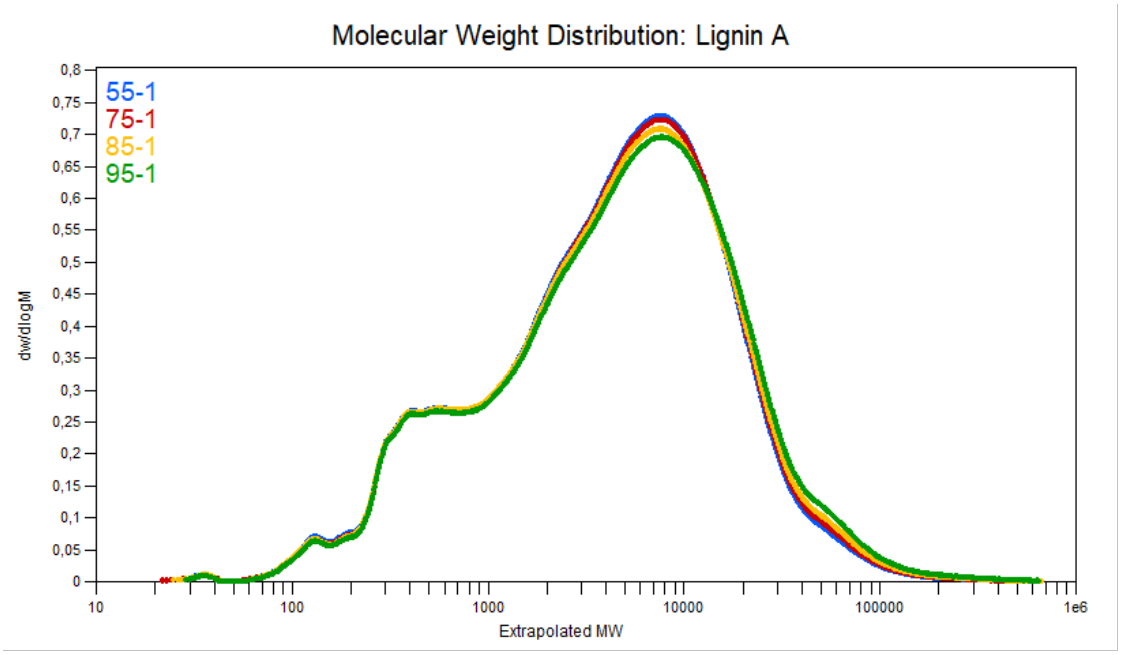

Figure 4.8: Chromatogram of lignin A samples treated at different temperatures.

4.3.2 Molecular structure

There are numerous types of linkages present in the lignin macromolecule, and because of this heterogeneity, extensive changes in the structure can occur during thermal treatment. NMR enables for elucidation of any molecular alterations of lignin with high precision, as well as quantifying them.

Listed in Table 4.6 are various lignin moieties along with the amounts per 100 aromatic units in lignin A. Additionally, all spectra are shown in Appendix B. These indicate that there is a distinct increment in the degree of condensation upon thermal treatment of lignin, which is related to the decline of protonated aromatic carbons (Ar-H). This indicates that polymerization reactions possibly initiated by radicals occur during thermal treatment, with a positive correlation between temperature and extent of reaction, and an onset already before 75°C. There is however no clear trend in the amount of β-O-4 linkages, despite the relatively low bond dissociation energy of 274.0 kJ mol^{-1} [34]. Additionally, this is consistent with the GPC measurements, where an increase in molecular weight with elevated treatment temperature was seen, possibly correlating to more condensation and less cleavage of intramolecular linkages.

Moreover, a drop in carbohydrates (C_1) content is seen with increasing treatment temperature. The reduction is most likely due to reactive glycosidic bonds in the carbohydrates getting cleaved as this hydrolytic reaction is acid catalyzed. The residues would then be dissolved in the filtrate, passing through the filter paper. Carbohydrates might be covalently bound to lignin, making it less hydrophobic and thus weakening the repulsion between the solid and liquid phase. In this case where carbohydrate content decreases, it is possible that the particles become more

hydrophobic, which enhances the separation from the polar liquid medium that is water.

It should be mentioned that the quantification of both β-O-4 and carbohydrates (C_1) in ^{13}C NMR were found to be highly sensitive to baseline correction; even minuscule adjustments yielded very different values. Further investigation into β-O-4 and carbohydrate contents was done by HSQC analysis, detailed in Appendix C. Further, thermal treatment does not seem to change the composition of functional groups detectable with the employed NMR methods, namely hydroxyl, carbonyl, and ester groups. Hence, from these results, it is not possible to elucidate if there is a structural change in the surface chemistry of the particle that explains the decrease in ζ potential with increasing treatment temperature.

Table 4.6: Amounts of lignin moieties per 100 Ar in lignin A quantified with ^{13}C NMR. Non-acetylated samples are referred to as *na*, and acetylated ones as *ac*.

Structure	**Quantification**	**55°C**	**75°C**	**85°C**	**95°C**
β-O-4	$(I_{90-82.5})_{na}$-$(I_{90-82.5})_{ac}$	2.90	3.84	2.91	4.65
Carbohydrates (C_1)	$(I_{102-98})_{ac}$	2.14	1.89	1.20	0.80
Et-O (Extractives)	$[(I_{16.5-13})_{ac}+(I_{16.5-13})_{na}]/2$	7.25	6.90	6.96	7.58
OMe	$[(I_{58-54})_{ac}+(I_{58-54})_{na}]/2$	82.14	82.59	82.52	83.76
ArH	$(I_{127.1-102})_{ac}$	209.16	205.40	198.94	196.28
Degree of condensation	(200+OMe)-ArH	72.98	77.19	83.58	87.48
Primary aliphatic OH	$(I_{172-169.7})_{ac}$-$(I_{172-169.7})_{na}$	35.47	35.74	39.11	38.26
Secondary aliphatic OH	$(I_{169.7-168.7})_{ac}$-$(I_{169.7-168.7})_{na}$	21.56	21.49	23.06	23.77
5-free phenolic OH	$(I_{168.7-168.3})_{ac}$-$(I_{168.7-168.3})_{na}$	34.61	34.96	35.77	25.64
5-subst. phenolic OH	$(I_{168.3-166})_{ac}$-$(I_{168.3-166})_{na}$	36.31	34.93	30.14	40.98
Non-conjugated CO	$[(I_{215-200})_{ac}+(I_{215-200})_{na}]/2$	8.30	6.67	5.31	7.45
Conjugated CO	$[(I_{200-185})_{ac}+(I_{200-185})_{na}]/2$	7.29	6.64	4.14	8.82
Non-conjugated COOR	$(I_{178-168.5})_{na}$	16.94	15.48	15.20	15.14
Conjugated COOR	$(I_{168.5-165})_{na}$	1.44	1.34	1.24	1.16

4.4 Thermal properties

Thermal properties refer to the characteristics of a material that determine how it responds to changes in temperature, which could be connected to the structure of

the molecule, especially when considering polymers like lignin.

4.4.1 Differential scanning calorimetry (DSC)

DSC was conducted to further gain knowledge about how the treatments affected the samples in terms of thermal stability and change in T_g, which can also help strengthen conclusions drawn from NMR results. Variation in T_g can suggest differences in cross-linking, molecular weight and presence of different functional groups. The DSC instrument was programmed in a Heat/Cool/Heat manner, in order to eliminate any prior thermal history by initially heating the material above a significant transition point (such as glass transition or melting), allowing for relaxation or molecular rearrangement. The material is then cooled at a controlled rate before being reheated, ensuring any effects from previous thermal cycles are removed.

Presented in Figure 4.9 are DSC curves of lignins A and B. The first heating displays the occurrence of an endothermic event up to approximately 75°C. Even though all samples had been thoroughly freeze-dried prior to measurement, thin layers of water rapidly condense on the lignin particles when transferring samples. Since the upper limit of this endothermic event correspond to the boiling point of water, it can be reasonably concluded that these are related. Beyond 75°C, the curves indicate an exothermic event. It is, however, unclear exactly what it correlates to. Evidence from GPC and NMR suggest it is some sort of condensation or cross-linking reaction, both being exothermic. The slightly different shapes of the exothermic peak, and in the case of lignin A a shift in temperature interval, for the lignins treated at different temperatures also indicate deviations in their molecular structures possibly generated during the thermal treatment, due to different temperatures.

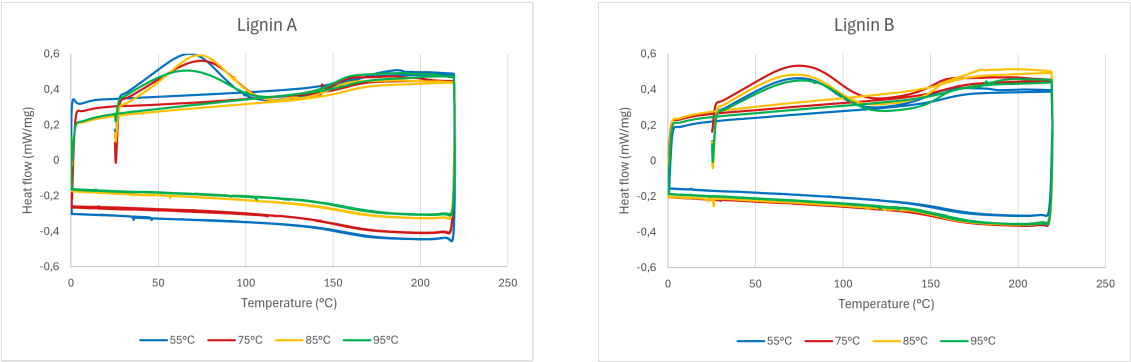

Figure 4.9: Endo up DSC heat/cool/heat curves of lignins A and B. The temperature cycle was programmed to first heat the sample from room temperature to 220°C, then cool down to 0°C, and finally heat back up to 220°C.

From DSC curves, it is also possible to determine the T_g of the lignin polymers. During a DSC heat/cool/heat experiment, as the material is heated, the T_g appears as an endothermic shift indicating the transition from a glassy state to a rubbery state. This shift is typically observed as a change in the heat capacity of the material, seen on the DSC curve as an inflection point. The temperature range in which this

change appears is around 140 to 170°C, and is seen both in the cooling and second heating. The T_g for all lignin samples were calculated and are shown in Table 4.7. All values are presented as the average T_g from the cooling and the second heating. It should be remembered that the T_g is a range of temperatures, and especially wide for a heterogenous polymer like lignin. The values presented in Table 4.7 is the inflection point of the range, meaning where the derivative has its maximum value. Heating lignin in the range 55 to 95°C, which are relatively mild conditions, does not seem to change the T_g of the lignin noteworthy. For lignin B, there is somewhat of a trend of increasing T_g with treatment temperature. This increment could be related to a supposed elevated M_w, assuming lignin B follows the behavior of lignin A regarding GPC results. Larger molecules have stronger intermolecular forces, which require more energy to break. Another explanation could be attributed to a higher degree of condensation, as it restricts molecular motion and makes the polymer more rigid. Again, this is under the assumption that lignin B behaves similarly to lignin A, as NMR has not been performed on lignin B.

Table 4.7: Calculated T_g from DSC data for lignins A and B.

Sample	**T_g (°C)**
55A	157.2
75A	156.5
85A	156.0
95A	158.5
55B	156.8
75B	157.5
85B	158.5
95B	158.9

4.5 Future work

Work on extending the understanding and knowledge on how and why thermal treatment of LignoBoost lignin affects its filtration properties has been carried out in this thesis. An extensive analytical characterization of structural and colloidal properties of particles was conducted. Nevertheless, there is still significant research needed to fully comprehend the effects of heat on lignin. Potential directions for future studies include:

- Optimizing the time needed for thermal treatment in order to increase both energy and filtration efficiency.
- Modeling how parameters such as temperature, duration of treatment and type of lignin influence filtration properties.
- Further investigating the reasons for why there is a significant difference in filtration efficiency between samples treated at 55 and 75 °C. One suggestion would be to perform BET and BJH analysis to investigate specific surface area and porosity.

5
Conclusion

Through an extensive characterization and analysis of colloidal, structural, and thermal properties of LignoBoost lignin following thermal treatment, several key findings have been revealed and connected to filtration properties.

Thermal treatment of LignoBoost lignin at 75, 85, and 95°C was seen to greatly improve filtration efficiency in terms of filtration time and dry content, when compared to a reference sample treated at 55°C. The reasons for these improved filtration properties can, according to the acquired results, mainly be attributed to changes in colloidal properties, which with certainty are connected to structural changes. An increase of particle size was observed with an onset at 85°C, which could also be visually verified with optical microscopy, where the smallest fraction of particles was seen to disappear between 75 and 85°C. This changed agglomeration behavior could possibly be related to the large drop in surface charge between these two treatment temperatures, causing a reduction in electrostatic repulsion and thus promoting particle agglomeration, leading to an increase in particle size. The cause of this change in surface charge is still unclear, but it might be linked to chemical reactions occurring above 75°C, altering the surface chemistry of the particle by decreasing charged groups. No drastic change in functional groups that could carry a charge was nevertheless discovered in the ^{13}C NMR results, even though a modest but consistent decrease in carboxylic groups and carbohydrates could be observed. However, they did reveal an increase in the degree of condensation, which was also corroborated by GPC measurements showing an increase in molecular weight.

Bibliography

[1] J. K. Weng and C. Chapple, "The origin and evolution of lignin biosynthesis," *New Phytologist*, vol. 187, pp. 273–285, 7 2010.

[2] F. J. B. Gomes, R. E. de Souza, E. O. Brito, and R. C. C. Lelis, "A review on lignin sources and uses," *Journal of Applied Biotechnology Bioengineering*, pp. 100–105, 5 2020.

[3] R. C. Sun, "Lignin source and structural characterization," *ChemSusChem*, vol. 13, pp. 4385–4393, 9 2020.

[4] M. Graglia, N. Kanna, and D. Esposito, "Lignin refinery: Towards the preparation of renewable aromatic building blocks," *ChemBioEng Reviews*, vol. 2, pp. 377–392, 12 2015.

[5] J. J. Liao, N. H. A. Latif, D. Trache, N. Brosse, and M. H. Hussin, "Current advancement on the isolation, characterization and application of lignin," *International Journal of Biological Macromolecules*, vol. 162, pp. 985–1024, 11 2020.

[6] "Lignin extraction process." [Online]. Available: https://www.valmet.com/pulp/other-value-adding-processes/lignin-extraction/lignoboost-process/

[7] H. Wallmo and A. Littorin, "Method and system for producing lignin," 2021.

[8] J. Durruty, T. Mattsson, and H. Theliander, "Local filtration properties of kraft lignin: The influence of residual xylan," *Separation and Purification Technology*, vol. 179, pp. 455–466, 5 2017.

[9] Y. Matsushita, C. Ko, D. Aoki, S. Hashigaya, S. Yagami, and K. Fukushima, "Enzymatic dehydrogenative polymerization of monolignol dimers," *Journal of Wood Science*, vol. 61, pp. 608–619, 12 2015.

[10] "Chemical and structural characterization of hardwood and softwood lignoforce™ lignins," *Industrial Crops and Products*, vol. 173, 12 2021.

[11] V. J. Hare and A. Lavergne, "Differences in carbon isotope discrimination between angiosperm and gymnosperm woody plants, and their geological significance," *Geochimica et Cosmochimica Acta*, vol. 300, pp. 215–230, 5 2021.

[12] R. Katahira, T. J. Elder, and G. T. Beckham, "A Brief Introduction to Lignin Structure," in *Lignin Valorization: Emerging Approaches*. The Royal Society of Chemistry, 04 2018. [Online]. Available: https://doi.org/10.1039/9781788010351-00001

[13] C. Crestini, H. Lange, M. Sette, and D. S. Argyropoulos, "On the structure of softwood kraft lignin," *Green Chemistry*, vol. 19, p. 4104, 2017. [Online]. Available: http://www.knowpulp.com

[14] "An overview on the use of lignin and its derivatives in fire retardant polymer systems," *Lignin - Trends and Applications*, 3 2018.

[15] G. Gellerstedt, "Softwood kraft lignin: Raw material for the future," *Industrial Crops and Products*, vol. 77, pp. 845–854, 12 2015.

[16] K. A. Y. Koivu, H. Sadeghifar, P. A. Nousiainen, D. S. Argyropoulos, and J. Sipilä, "Effect of fatty acid esterification on the thermal properties of softwood kraft lignin," *ACS Sustainable Chemistry Engineering*, vol. 4, pp. 5238–5247, 10 2016.

[17] P. Maijala, "Heterobasidion annosum and wood decay: Enzymology of cellulose, hemicellulose, and lignin degradation," 01 2000.

[18] O. Yu and K. H. Kim, "Lignin to materials: A focused review on recent novel lignin applications," *Applied Sciences (Switzerland)*, vol. 10, 7 2020.

[19] N. Brosse, R. El Hage, M. Chaouch, M. Pétrissans, S. Dumarçay, and P. Gérardin, "Investigation of the chemical modifications of beech wood lignin during heat treatment," *Polymer Degradation and Stability*, vol. 95, no. 9, pp. 1721–1726, 2010. [Online]. Available: https://www.sciencedirect.com/science/article/pii/S0141391010002077

[20] J.-Y. Kim, H. Hwang, S. Oh, Y.-S. Kim, U.-J. Kim, and J. W. Choi, "Investigation of structural modification and thermal characteristics of lignin after heat treatment," *International Journal of Biological Macromolecules*, vol. 66, pp. 57–65, 2014. [Online]. Available: https://www.sciencedirect.com/science/article/pii/S014181301400097X

[21] T. T. Nge, Y. Tobimatsu, M. Yamamura, S. Takahashi, E. Takata, T. Umezawa, and T. Yamada, "Effect of heat treatment on the chemical structure and thermal properties of softwood-derived glycol lignin," *Molecules*, vol. 25, no. 5, 2020. [Online]. Available: https://www.mdpi.com/1420-3049/25/5/1167

[22] J. Wojtasz-Mucha, M. Hasani, and H. Theliander, "Dissolution of wood components during hot water extraction of birch," *Wood Science and Technology*, vol. 55, pp. 811–835, 5 2021.

[23] ——, "Dissolution of wood components during hot water extraction of spruce," *TAPPI JOURNAL*, vol. 22, 2023.

[24] A. Hjorth, A. V. Kristiansen, H. H. Øvrebø, and H. Theliander, "Electro-assisted filtration of microfibrillated cellulose: the impact of the degree of fibrillation," *Cellulose*, vol. 30, pp. 10 097–10 116, 11 2023.

[25] H. Ohshima, *Electrical Double Layers*. Berlin, Heidelberg: Springer Berlin Heidelberg, 2013, pp. 342–361. [Online]. Available: https://doi.org/10.1007/978-3-642-20665-8_15

[26] S. Lorenzen, K. Keiding, and M. L. Christensen, "The effect of particle surface charge density on filter cake properties during dead-end filtration," *Chemical Engineering Science*, vol. 163, pp. 155–166, 2017. [Online]. Available: https://www.sciencedirect.com/science/article/pii/S0009250917300659

[27] R. Wakeman, "The influence of particle properties on filtration," *Separation and Purification Technology*, vol. 58, pp. 234–241, 12 2007.

[28] L. Wang, X. Yang, Q. Wang, Y. Zeng, L. Ding, and W. Jiang, "Effects of ionic strength and temperature on the aggregation and deposition of multi-walled carbon nanotubes," *Journal of Environmental Sciences*, vol. 51, pp. 248–255, 2017. [Online]. Available: https://www.sciencedirect.com/science/article/pii/S1001074216302443

[29] F. M. Tiller and J. H. Kwon, "Role of porosity in filtration: Xiii. behavior of highly compactible cakes," *AIChE Journal*, vol. 44, pp. 2159–2167, 1998.

[30] R. Wakeman and E. S. Tarleton, *Solid/liquid separation: principles of industrial filtration*. Elsevier, 2005.

[31] "Identification of a diagnostic structural motif reveals a new reaction intermediate and condensation pathway in kraft lignin formation," *Chemical Science*, vol. 9, pp. 6348–6360, 8 2018. [Online]. Available: https://pubs.rsc.org/en/content/articlehtml/2018/sc/c8sc02000khttps://pubs.rsc.org/en/content/articlelanding/2018/sc/c8sc02000k

[32] M. Y. Balakshin and E. A. Capanema, "Comprehensive structural analysis of biorefinery lignins with a quantitative 13 c nmr approach †," 2015. [Online]. Available: https://pubs.rsc.org/en/content/articlelanding/2015/ra/c5ra16649g

[33] E. V. Ramana and A. Mahajan, "Patents on magnetoelectric multiferroics and their processing by electrophoretic deposition," *Recent Patents on Materials Science*, vol. 7, pp. 109–130, 05 2014.

[34] C. Zhang, J. Lu, X. Zhang, K. E. MacArthur, M. Heggen, H. Li, and F. Wang, "Cleavage of the lignin β-o-4 ether bond via a dehydroxylation–hydrogenation strategy over a nimo sulfide catalyst," *Green Chemistry*, vol. 18, pp. 6545–6555, 2016. [Online]. Available: https://api.semanticscholar.org/CorpusID:100568130

A

d-values of the particle size distributions

Table A.1: d-values of lignin A, measured as the number based size distribution. Samples are named according to temperature_treatment duration (min)_number percentage.

Sample (Lignin A)	d (0,1)	d (0,5)	d (0,9)
55_t0_n	1,2	1,6	3,4
55_t15_n	1,2	1,6	3,6
55_t30_n	1,2	1,6	3,6
55_t45_n	1,2	1,7	3,6
55_t60_n	1,2	1,7	3,7
75_t0_n	1,2	1,6	3,0
75_t15_n	1,2	1,7	2,9
75_t30_n	1,2	1,7	3,0
75_t45_n	1,3	1,7	3,1
75_t60_n	1,3	1,9	3,3
85_t0_n	1,3	1,8	3,2
85_t15_n	1,6	2,8	6,5
85_t30_n	1,7	3,2	7,3
85_t45_n	1,7	3,2	7,4
85_t60_n	1,8	3,3	7,6
95_t0_n	3,4	5,5	10,4
95_t15_n	3,6	5,8	10,8
95_t30_n	3,6	5,7	10,7
95_t45_n	3,5	5,7	10,7
95_t60_n	3,5	5,7	10,6

Table A.2: d-values of lignin A, measured as the volume based size distribution. Samples are named according to temperature_treatment duration (min)_volume percentage.

Sample (Lignin A)	d (0,1)	d (0,5)	d (0,9)
55_t0_v	3,7	12,0	24,8
55_t15_v	4,0	11,9	23,4
55_t30_v	3,9	11,7	23,0
55_t45_v	3,8	11,8	23,6
55_t60_v	3,8	11,6	22,9
75_t0_v	3,2	11,8	24,4
75_t15_v	2,1	11,0	23,0
75_t30_v	2,2	10,9	23,3
75_t45_v	2,3	9,4	22,0
75_t60_v	2,1	10,0	22,7
85_t0_v	2,2	10,9	24,2
85_t15_v	4,1	10,8	22,9
85_t30_v	4,5	11,1	23,1
85_t45_v	4,7	11,4	23,8
85_t60_v	4,8	11,2	22,8
95_t0_v	5,5	11,6	24,1
95_t15_v	6,2	12,2	24,4
95_t30_v	6,2	12,1	23,8
95_t45_v	6,2	12,2	24,5
95_t60_v	6,1	12,0	23,4

Table A.3: d-values of lignin B, measured as the number based size distribution. Samples are named according to temperature_treatment duration (min)_number percentage.

Sample (Lignin B)	d (0,1)	d (0,5)	d (0,9)
55_t0_n	1,0	1,5	3,0
55_t15_n	1,0	1,5	3,0
55_t30_n	1,0	1,5	3,0
55_t45_n	1,0	1,5	3,0
55_t60_n	1,0	1,5	3,0
75_t0_n	1,0	1,5	3,0
75_t15_n	1,1	1,5	3,0
75_t30_n	1,2	1,6	3,2
75_t45_n	1,2	1,7	3,2
75_t60_n	1,2	1,6	3,2
85_t0_n	1,2	1,7	3,4
85_t15_n	1,8	3,0	6,3
85_t30_n	2,5	4,0	8,1
85_t45_n	3,3	5,2	10,2
85_t60_n	3,0	4,8	9,3
95_t0_n	3,8	6,0	11,5
95_t15_n	8,4	12,6	22,9
95_t30_n	8,5	12,6	22,9
95_t45_n	8,8	13,1	23,8
95_t60_n	8,7	13,1	23,8

Table A.4: d-values of lignin B, measured as the volume based size distribution. Samples are named according to temperature_treatment duration (min)_volume percentage.

Sample (Lignin B)	d (0,1)	d (0,5)	d (0,9)
55_t0_v	3,0	17,7	56,5
55_t15_v	2,9	17,5	55,9
55_t30_v	3,0	17,5	55,8
55_t45_v	2,7	15,0	51,8
55_t60_v	2,7	14,9	49,2
75_t0_v	2,9	16,8	52,9
75_t15_v	3,0	17,5	54,9
75_t30_v	2,9	16,9	53,5
75_t45_v	2,9	16,9	54,7
75_t60_v	2,8	16,0	51,9
85_t0_v	3,0	17,7	56,8
85_t15_v	4,4	18,5	64,6
85_t30_v	5,3	21,2	74,1
85_t45_v	6,0	19,6	71,2
85_t60_v	5,9	21,4	73,2
95_t0_v	6,5	22,1	82,2
95_t15_v	12,9	29,4	95,6
95_t30_v	13,2	29,0	86,6
95_t45_v	13,7	29,6	80,4
95_t60_v	13,8	29,8	81,2

B

^{13}C NMR spectra

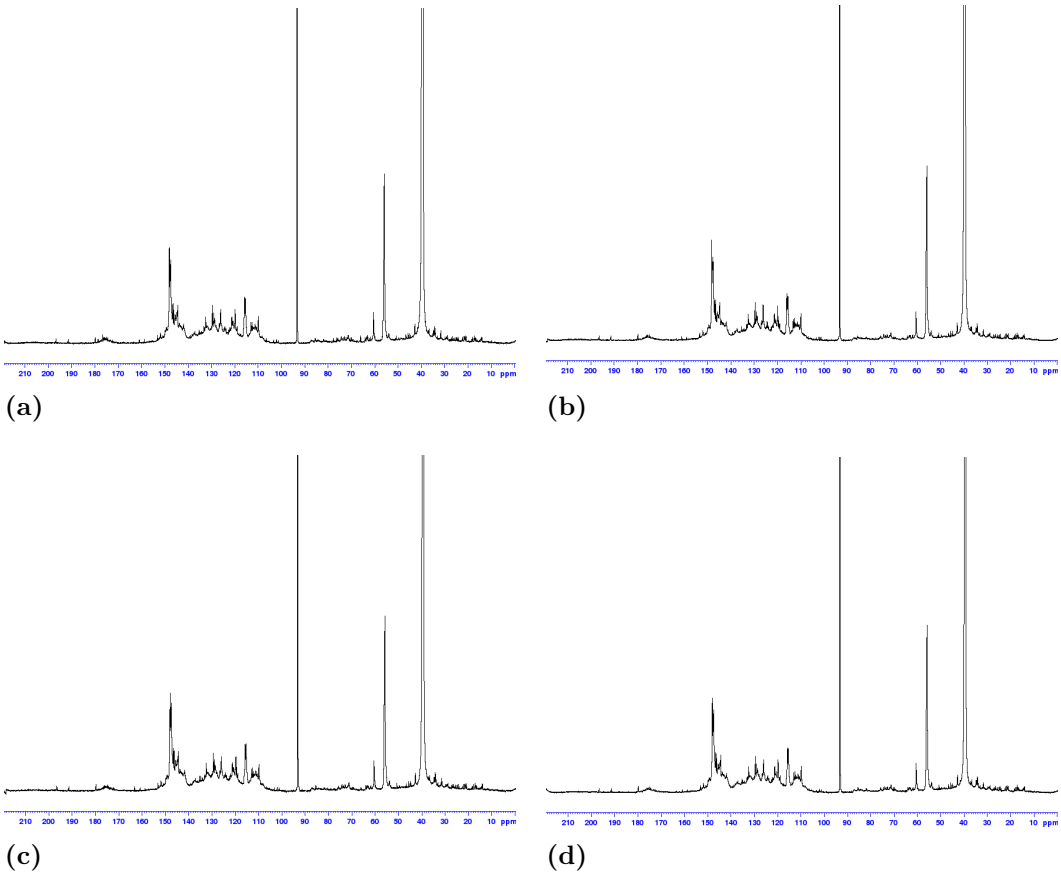

Figure B.1: ^{13}C NMR spectra of non-acetylated lignin A samples treated at (a) 55°C, (b) 75°C, (c) 85°C, and (d) 95°C.

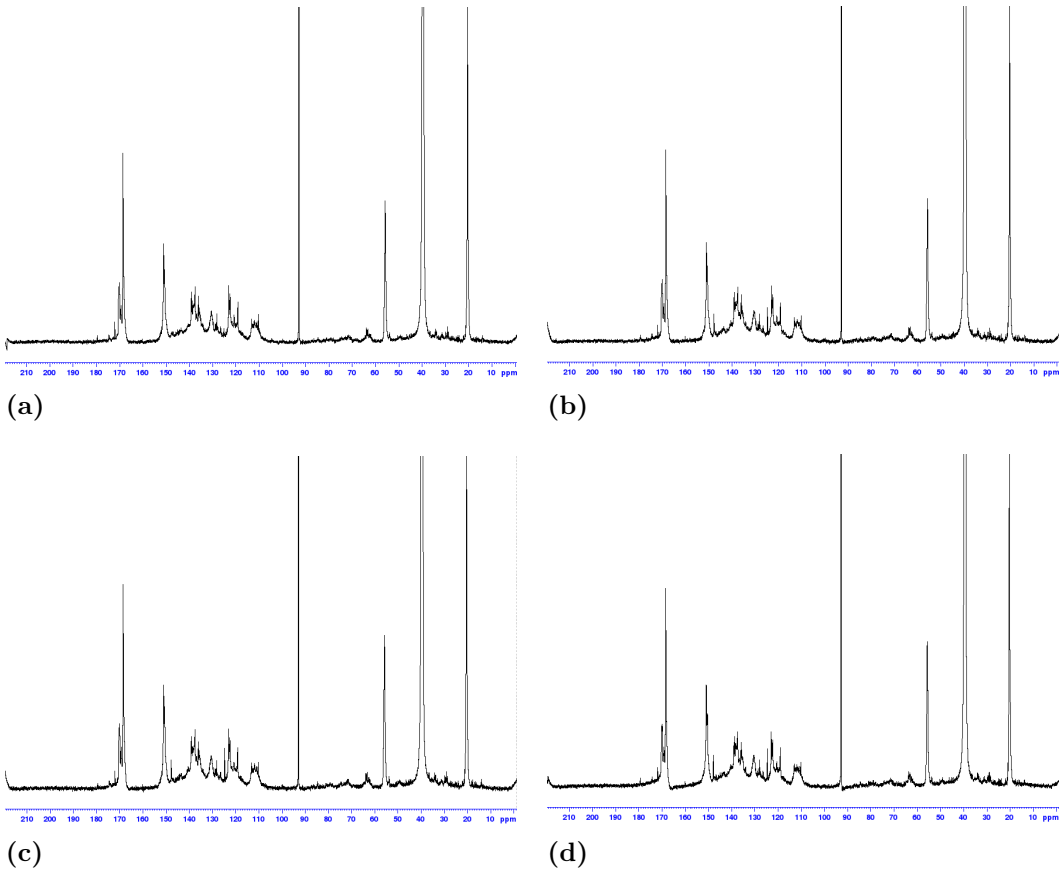

Figure B.2: ^{13}C NMR spectra of acetylated lignin A samples treated at (a) 55°C, (b) 75°C, (c) 85°C, and (d) 95°C.

C

HSQC spectra

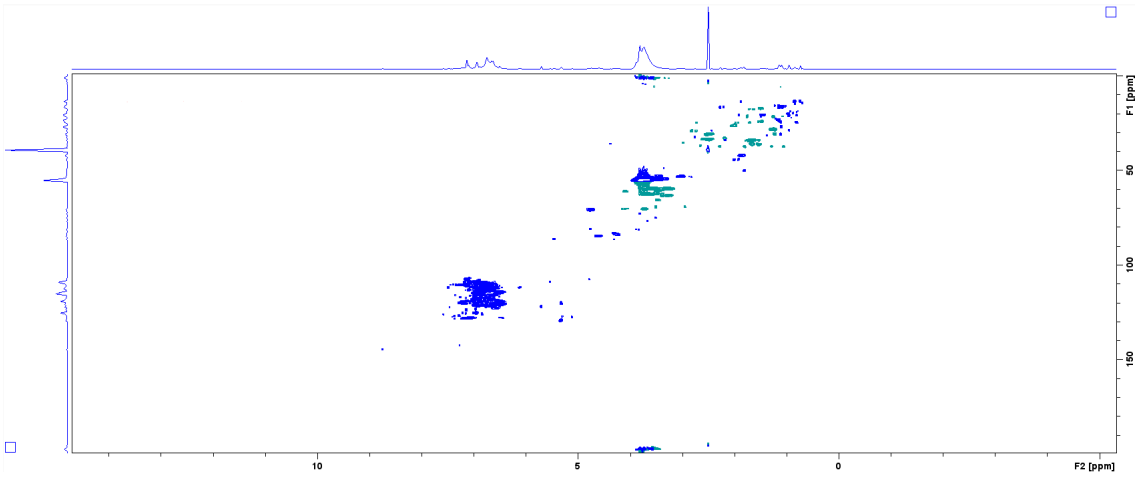

Figure C.1: HSQC spectrum of lignin A after thermal treatment at 55°C.

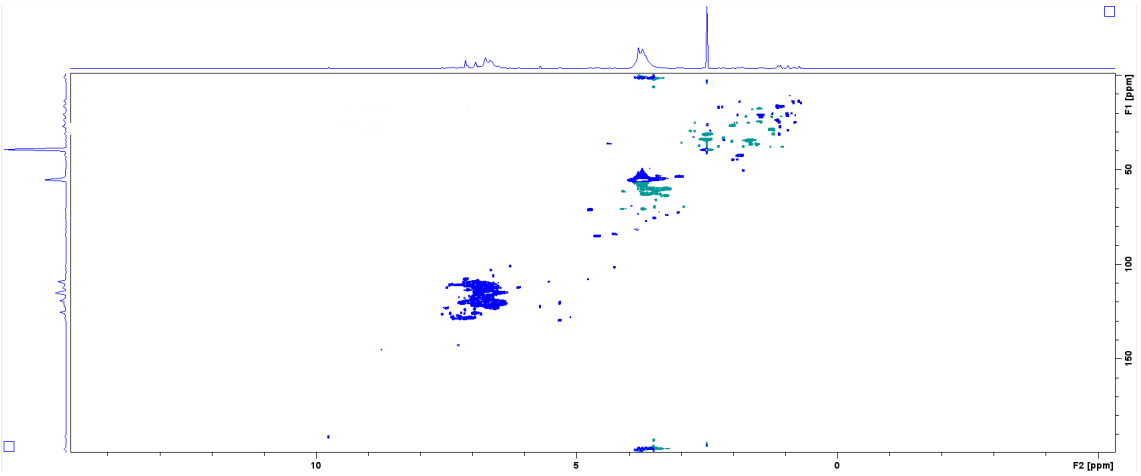

Figure C.2: HSQC spectrum of lignin A after thermal treatment at 95°C.

Table C.1: Amounts of lignin moieties per 100 Ar in lignin A quantified with HSQC 2D NMR.

Structure	**55°C**	**95°C**
β-O-4	3.29	3.30
β-β	2.34	3.18
β-5	1.08	0.92
Xylan	0.38	0.95

DEPARTMENT OF FOREST PRODUCTS AND CHEMICAL ENGINEERING
CHALMERS UNIVERSITY OF TECHNOLOGY
Gothenburg, Sweden
www.chalmers.se

CHALMERS
UNIVERSITY OF TECHNOLOGY